CUSTOMIZABLE SURFACE RESISTANCE OF RESISTIVE FSS USING INKJET PRINTING TECHNOLOGY

S.N. Zabri[1*], M.A. Meor Said[1], U. R. Hashim[2], and L. Salahuddin[2]

[1]Faculty of Electronics and Computer Technology and Engineering (FTKEK), Microwave Research Group (MRG), Centre for Telecommunication Research & Innovation (CeTRI), Universiti Teknikal Malaysia Melaka, 76100, Durian Tunggal, Melaka, Malaysia.

[2]Faculty of Information & Communication Technology Universiti Teknikal Malaysia Melaka Hang Tuah Jaya, 76100 Durian Tunggal Melaka, Malaysia.

* normi@utem.edu.my

Article History: Received xxxxx; Revised xxxx; Accepted xxxx

ABSTRACT: This paper reports on a new manufacturing strategy that offers a low-cost, simple, and repeatable method for printing frequency selective surface (FSS) elements using materials with slightly lower conductivity than metals. By employing an inkjet printer to simultaneously pattern the FSS elements on the substrate and digitally control the dot density of the nanosilver ink mixture and aqueous vehicle, surface resistances can be achieved much closer to the desired values compared to the stencil printing method.

KEYWORDS: *Inkjet Printing; Printed Electronics; Surface Resistance; Flexible Electronics; FSS*

1.0 INTRODUCTION

The global electronics industry is increasingly demanding devices that are smaller, lighter, and more cost-effective to manufacture than previous models. In recent years, printed electronics technology has been utilized for constructing various components such as Coplanar Waveguide (CPW) Lines [1], RFID tags [2], antennas [3] – [6], FSS [7, 8] and sensors [9] – [12]. This approach helps reduce costs associated with conventional fabrication methods by enabling direct printing from a computer, thereby eliminating the need for photolithography and milling and reducing production time [13, 14]. Additionally, material waste is minimized by printing only the required patterns or areas [15]. All the applications mentioned above employ conductive ink which is delivered through a printer.

Moreover, this method presents an advantageous approach for manufacturing thin microwave absorbers. Recently, an inkjet printing technology was employed to fabricate a metal-backed resistively loaded Frequency Selective Surface (FSS) [8]. The FSS pattern, featuring a surface resistance using conductive ink. The absorber design is based on the use of a lossy substrate and therefore only requires a very small surface resistance to construct the FSS elements. In certain applications, utilizing high conductivity metals for creating resonant elements within periodic arrays [12], [13] may not be desirable, demanding selective patterning of materials exhibiting a surface resistance higher than that of commercially available conductive inks. This paper introduces an alternative printing strategy utilizing an inkjet printer to simultaneously pattern elements with a single value of surface resistance and uniform ink thickness at once.

2.0 INKJET PRINTING OF RESISTIVE FSS

The study utilizes a desktop color inkjet printer, specifically the Epson Stylus C88+, equipped with CMYK (Cyan, Magenta, Yellow, Black) cartridges and MicroPiezo technology. This printer operates by delivering ink droplets through a piezoelectric head, achieving resolutions of 360 dots per inch in both vertical and horizontal planes. Unlike thermal inkjet printers that rely on vapor bubble formation as depicted in Figure 1, the piezoelectric technology allows for the use of various types of solvent-based inks [13], enhancing versatility. The monochrome head features 180 nozzles, while the color head has 177 nozzles (59 for each CMY color), enabling the production of three different sizes of ink droplets, with a minimum volume of 3 picoliters (pL). These droplets are deposited on flexible substrates with dimensions up to A4 size and thicknesses of up to 0.27 mm.

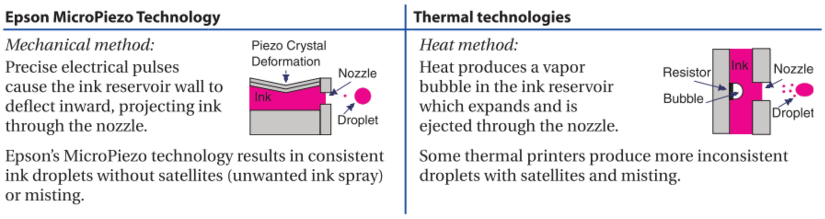

Figure 1: Comparison the comparison of inkjet technology methods [14].

For printing FSS elements, Metalon™ JS-B25P nanosilver ink and Metalon™ aqueous vehicle from Novacentrix are utilized in varying volume ratios. The JS-B25P ink is electrically conductive, containing 25 wt% Ag, and is formulated to achieve thin film sheet resistances as low as 60 milliohm/square. This ink type has previously been employed in printing solar cell antennas. The aqueous vehicle, used to clean the printer head and prevent blockages, is also water-based but significantly less conductive, containing 5 – 10 wt% Ethylene glycol and Glycerine.

Several common color models or parameters are available for modifying color characteristics within patterns. These include RGB (Red, Green, Blue), black and white, greyscale, CMYK (Cyan, Magenta, Yellow, Black), Lab (Luminance, a & b for chrominance), HSL/V (Hue, Saturation, Lightness/Value), indexed, and web-safe colors. The selection of a specific model depends on the desired output or application. However, for this study, only RGB and CMYK models are used to simplify the study of the ink by reducing the number of parameters involved.

2.1 Colour Model

When working with a standard inkjet color printer equipped with four different color cartridges, understanding the color model is essential. A color model is defined as a set of colors systematically organized to be interpreted by computers. While numerous color models exist, the most prevalent are RGB and CMYK.

RGB serves as a color model primarily used for computer display, where Red, Green, and Blue are fundamental colors of light. These colors are combined in varying intensities to generate secondary colors. In computer systems, each color's intensity is represented by a numerical code ranging from 0 (no light) to 255 (full intensity).

Conversely, CMYK is a color model tailored for printing, where each color component mixes to produce both primary and secondary colors in the RGB spectrum. Similar to RGB, CMYK colors are represented numerically, typically ranging from 0 to 1 (100%). These color models (RGB and CMYK) are interconnected through combinations of two or more colors.

2.2 CMYK to RGB Conversion

Understanding the relationship between the color models RGB and CMYK is crucial for two main reasons:

i. Not all software platforms offer the capability to set CMYK values directly. Therefore, it is necessary to identify corresponding RGB values to ensure accurate color representation.
ii. If colour cartridges are to be used, it is simpler to identify a mixed ink ratio if a certain colour (surface resistance in this work) is required.

The red (R), green (G), and blue (B) components can be calculated using either online converters or the following equations:

$$R = 255 \times (1 - C) \times (1 - K) \quad (1)$$
$$G = 255 \times (1 - M) \times (1 - K) \quad (2)$$
$$B = 255 \times (1 - Y) \times (1 - K) \quad (3)$$

Here, K represents black. These equations illustrate that adjusting any RGB color component affects the primary color. Additionally, it demonstrates the possibility of using a single CMYK color to produce various shades of a similar color. This capability allows CMYK printers to potentially utilize a single cartridge (if individual selection is feasible) for printing patterns.

2.3 RGB and Dot Density

In addition to generating various colors perceivable by the human eye, the RGB model fundamentally represents the concentration of primary colors as dots. For instance, pure black and light gray, despite sharing identical black color values (and RGB values), they differ in dot concentration. This distinction was demonstrated by printing an identical rectangular pattern with varying RGB values using a Canon monochrome laser printer equipped with standard toner ink. The dot concentrations were examined using a Zeiss Stemi DV4 microscope, with results for three different RGB values depicted in Figure 2.

The images reveal that for a solid black color (RGB 0,0,0), the pattern received the maximum number of dots, making it challenging to discern the highly concentrated dots. Conversely, when RGB values were increased to (50,50,50), the dot arrangement became more distinct as fewer dots were deposited (white dots indicating no or minimal ink deposition). Similarly, at higher RGB values such as (100,100,100), fewer dots were printed, further illustrating the relationship between RGB values and dot density. In printed electronics, the number of dots that are used to print the pattern, determines the conductivity of the ink.

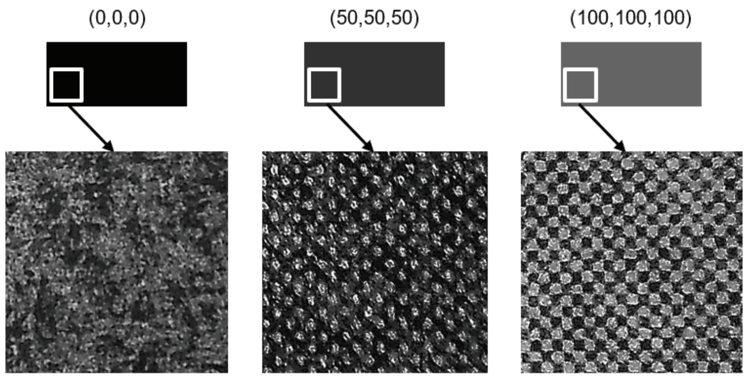

Figure 2: Optical microscope image of the dot concentration of rectangular patterns printed using a monochrome laser printer for 3 different RGB values

2.3 Printing Process and Settings

The printer utilized in this study is equipped with four cartridges (CMYK). During the printing process, it is sufficient to fill only the K cartridge with nano-silver ink. However, to prevent damage to the printer head, it is necessary to fill the remaining CMY cartridges with the aqueous vehicle, as all four cartridges are used and consume ink during the head cleaning process. The nano-silver ink and aqueous vehicle are deposited into the cartridges using a syringe, as illustrated in Figure 3.

Figure 3: Nano-silver ink and aqueous vehicle filling process into the CMYK empty cartridges of an Epson Stylus C88+ inkjet printer

3.0 EXPERIMENTAL VALIDATION

CST Microwave Studio software was employed to determine the physical dimensions of a periodic array of copper dipoles, designed to resonate at 15.3 GHz when exposed to TE (vertically) polarized waves at normal incidence.

An experiment was conducted to determine the dot concentration and ink composition required to achieve specific surface resistance values for loading the FSS elements. This process involved experimental testing and modification of the ink to slightly reduce its conductivity by:

i. reducing the dot concentration of the printed features.
ii. adding one or more liquid additives.

In this study, a 15×15 cm^2 array of linear dipoles was patterned on a 0.14 mm thick Novele IJ-220 substrate using the Epson Stylus C88+ inkjet printer and were printed with three different ink mixture volume ratio of (ink_{mL}: aqueous $vehicle_{mL}$) 1:5, 1:7 and 1:9 and various RGB settings.

The surface resistance in the numerical model was adjusted to achieve the best fit with the measured transmission and reflection response plots of inkjet-printed FSS with identical dimensions.

The measured transmission coefficients were plotted over the frequency range of 9 – 18 GHz for each of the three ink mixtures and various RGB color modes that resulted in a null depth greater than 5 dB at resonance (16 in total). These experimental results were compared with numerical predictions obtained by adjusting the surface resistance of the dipoles in the electromagnetic simulator to achieve the best fit. Figure 4 illustrates the measured spectral transmission plots for the three ink mixtures alongside the numerical results, including the corresponding surface resistance values. The RGB printer settings were varied between (0,0,0) and (27,27,27). It is observed that the surface resistance can be increased by reducing the dot density and/or the fraction of silver nano particles in the ink composition, and moreover it is possible to engineer the same resistance by choosing different combinations of these two print variables. Excellent agreement with the predicted reflectivity plot is observed thereby confirming that inkjet printing provides a better means than stencil printing, to tightly control the surface resistance value of the FSS elements.

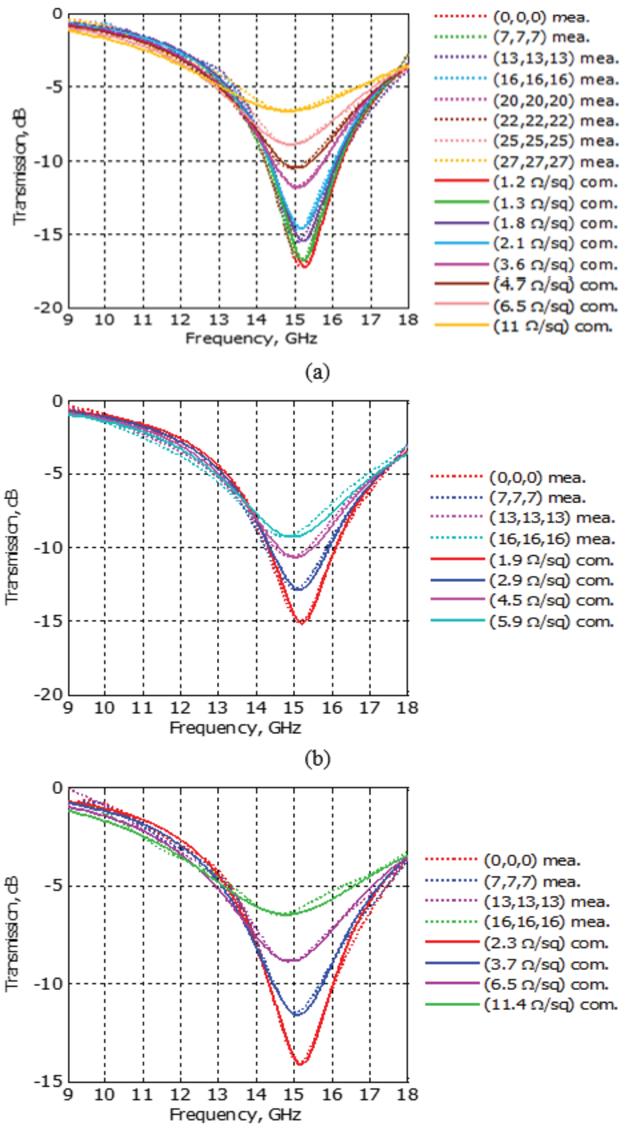

Figure 4: Measured spectral transmission plots of inkjet printed FSS at normal incidence and best fit simulated data for different RGB values of (a) 1:5 mixture, (b) 1:7 mixture, (c) 1:9 mixture

4.0 CONCLUSION

An important outcome from this work is the demonstration of a new alternative manufacturing strategy which provides a low cost, simple and repeatable means to solve this problem. By employing an ink-jet printer to simultaneously pattern the FSS elements on the substrate and digitally control the dot density of the solvent and nanosilver ink mixture, it is shown that it is possible to obtain surface resistances that are much closer to the desired values for optimum FSS performance. Numerical predictions are fitted to experimental transmission and reflection response plots of inkjet printed dipole FSS arrays, constructed using three different ink mixtures and features printed with nine different dot densities. It is shown that surface resistance values in the range of 0.1 – 200 Ω/sq are obtainable.

ACKNOWLEDGMENTS

The authors would like to acknowledge the support from the Faculty's Research Fund (Faculty of Electronics and Computer Technology and Engineering), Microwave Research Group (MRG), a research group under the Centre for Telecommunication Research & Innovation (CeTRI), Universiti Teknikal Malaysia Melaka (UTeM)..

REFERENCES

[1] O. Azucena, J. Kubby, D. Scarbrough, and C. Goldsmith, "Inkjet printing of passive microwave circuitry," in *IEEE MTT-S International Microwave Symposium Digest*, Atlanta, 2008.

[2] A. Rida, "Conductive inkjet-printed antennas on flexible low-cost paper-based substrates for RFID and WSN applications," M.S. Thesis, School of Electrical and Computer Engineering, Georgia Institute of Technology, 2009.

[3] A. Shastri, B. Sanz-Izquierdo, and S. Gao, "Manufacturing Considerations for the Development of Reconfigurable Antennas Using Inexpensive Inkjet Printing," *IEEE Transactions on Components, Packaging and Manufacturing Technology,* vol. 12, no. 6, pp. 1021-1028, 2022.

[4] A. Shastri, P. Njogu, B. Sanz-Izquierdo, S. Gao and Z. Chen, "Evaluation of Planar Inkjet-Printed Antennas on a Low-Cost Origami Flapping Robot," *IEEE Access,* vol. 8, pp. 164103-164113, 2020.

[5] A. R. Hossain, M. S. I. Sagar, A. A. Mertvyy, P. K. Sekhar and T. Karacholak, "Inkjet Printed Flexible Dual-Band Dual-Sense Circularly Polarized Patch Antenna," *IEEE Access,* vol. 12, pp. 55424-55433, 2024.

[6] U. Myrzakhan, F. A. Ghaffar, M. Vaseem, H. Fariborzi and A. Shamim, "Inkjet-Printed Ferrite Substrate-Based Vialess Waveguide Phase Shifter," *IEEE Transactions on Magnetics,* vol. 59, no. 4, p. 4000212, 2023.

[7] A. Shastri, P. Njogu, B. Sanz-Izquierdo, S. Gao and Z. Chen, "Low-cost Inkjet Printed Paper Poster FSS for 5G Applications," in *15th European Conference on Antennas and Propagation (EuCAP),* Dusseldorf, Germany, 2021.

[8] M. M. Gupta and N. Tirkey, "Inkjet-printed broadband FSS-based absorber with improved absorption characteristics," *International Journal of Microwave and Wireless Technologies,* pp. 1-9, 2023.

[9] O. O. Olowo, R. Zhang, J. Lin, D. Wei, A. Sherehiy, D. Jackson, D. Ratnayake, A. Tofangchi and D. O. Popa, "Design and Fabrication of an Aerosol Jet Printed Tactile Sensor on Flexible Substrate," *IEEE Journal on Flexible Electronics,* vol. 2, no. 2, pp. 190-200, 2023.

[10] Y. Sui, L. P. Kreider, K. M. Bogie, and C. A. Zorman, "Fabrication of a Silver-Based Thermistor on Flexible, Temperature-Sensitive Substrates Using a Low-Temperature Inkjet Printing Technique," *IEEE Sensors Letters,* vol. 3, no. 2, p. 2500704, 2019.

[11] Y. Huang, K. Chen, Y. Cheng, C. Lee and H. Tsai, "An Inkjet-Printed Flexible Non-Enzymatic Lactate Sensor for Clinical Blood Plasma Test," *IEEE Electron Device Letters,* vol. 41, no. 4, pp. 597-600, 2020.

[12] S. Gardner, A. Porbanderwala and M. R. Haider, "An Affordable Inkjet-Printed Foot Sole Sensor and Machine Learning for Telehealth Devices," *IEEE Sensors Letters,* vol. 7, no. 6, p. 6003304, 2023.

[13] M. A. Shah, D. Lee, B. Lee and S. Hur, "Classifications and Applications of Inkjet Printing Technology: A Review," *IEEE Access,* vol. 9, pp. 140079-140102, 2021.

[14] T. Tilford, S. Stoyanov, J. Braun, J. C. Janhsen, M. K. Patel and C. Bailey, "Comparative Reliability of Inkjet-Printed Electronics Packaging," *IEEE Transactions on Components, Packaging and Manufacturing Technology,* vol. 11, no. 2, pp. 351-362, 2021.

[15] A. Bastola, Y. He, J. Im, G. Rivers, F. Wang, R. Worsley, J. S. Austin, O. Nelson-Dummett, R. D. Wildman, R. Hague, C. J. Tuck and L. Turyanska, "Formulation of functional materials for inkjet printing: A pathway towards fully 3D printed electronics," *Materials Today Electronics,* vol. 6, p. 100058, 2023.